Article

Characterizing Urban Expansion Combining Concentric-Ring and Grid-Based Analysis for Latin American Cities

Su Wu [1], **Neema Simon Sumari** [2], **Ting Dong** [3], **Gang Xu** [4,5,*] and **Yanfang Liu** [1]

1. School of Resource and Environmental Sciences, Wuhan University, 129 Luoyu Road, Wuhan 430079, China; wusu027@whu.edu.cn (S.W.); yfliu610@163.com (Y.L.)
2. Department of Mathematics, Informatics and Computational Sciences, Solomon Mahlangu College of Science and Education, Sokoine University of Agriculture, P.O. Box 3038 Morogoro, Tanzania; neydsumari@sua.ac.tz
3. School of Geography and Tourism, Anhui Normal University, 189 Jiuhua South Road, Wuhu 241000, China; dongtingdt@whu.edu.cn
4. School of Remote Sensing and Information Engineering, Wuhan University, 129 Luoyu Road, Wuhan 430079, China
5. Key Laboratory of Urban Land Resources Monitoring and Simulation, Ministry of Natural Resources, 8007 West Hongli Road, Shenzhen 518034, China
* Correspondence: xugang@whu.edu.cn

Abstract: Spatio-temporal characterization of urban expansion is the first step towards understanding how cities grow in space. We summarize two approaches used in urban expansion measurement, namely, concentric-ring analysis and grid-based analysis. Concentric-ring analysis divides urban areas into a series of rings, which is used to quantify the distance decay of urban elements from city centers. Grid-based analysis partitions a city into regular grids that are used to interpret local dynamics of urban growth. We combined these two approaches to characterize the urban expansion between 2000–2014 for five large Latin American cities (São Paulo, Brazil; Mexico City, Mexico; Buenos Aires, Argentina; Bogotá, Columbia; Santiago, Chile). Results show that the urban land (built-up area) density in concentric rings decreases from city centers to urban fringe, which can be well fitted by an inverse S curve. Parameters of fitting curves reflect disparities of urban extents and urban form among these five cities over time. Grid-based analysis presents the transformation of population from central to suburban areas, where new urban land mostly expands. In the global context, urban expansion in Latin America is far less rapid than countries or regions that are experiencing fast urbanization, such as Asia and Africa. Urban form of Latin American cities is particularly compact because of their rugged topographies with natural limitations.

Keywords: urban expansion; concentric-ring analysis; grid-based analysis; invers S curve; Latin America

1. Introduction

More and more people are now living in cities, driving the persistent expansion of urban land across the world [1]. Rapid expansion of urban land swallows cultivated land and natural land, threatening biodiversity and exacerbating environmental degradation [2–4]. Numerous studies have investigated spatio-temporal characteristics of urban land expansion and its environmental consequences [5,6]. Remote sensing and geographical information science (GIS) have greatly contributed to quantifying land use changes [7]. Remotely sensed imagery provides the first-hand data used to monitor urban growth in space [8]. GIS-based technologies provide a wealth of tools for urban expansion measurement [9].

The first step to measure urban expansion is its speed and intensity, for instance, the annual growth rate of built-up areas [10,11]. The intensity of urban expansion refers to proportions of urban land use changes to the total land area in a defined region [10,12]. Beyond the statistical description of urban land use changes, the spatial perspective is employed to answer the spatial pattern of urban form and where the urban expansion happens [13]. Thirdly, the temporal process cannot be separated when we characterize

urban expansion [14]. Landscape metrics are broadly used to measure dynamics and heterogeneities in the temporal process of urban expansion [15]. Finally, urban theories behind urban land use changes are proposed based on these quantitative measurements, such as the diffusion-coalescence theory [16–18], pattern-process interrelationships, distance-decay of densities [19,20], types of urban expansion (infilling, extension, and leapfrog) [21–24], and driving forces of urban expansion [25], etc.

As far as the spatial unit is concerned, there are two approaches to quantify urban expansion, namely, the concentric-ring analysis and grid-based analysis [13,26]. The concentric-ring analysis, also known as gradient analysis, divides urban areas into a series of concentric rings from the city center, which usually is the point of origin or central business district (CBD) of the city [27,28]. The concentric-ring analysis is often used in conjunction with landscape metrics (such as the percent of landscape, patch density, and many other indicators) [12,22]. They are used to analyze spatial patterns (distance-decay) of urban landscape. The distance-decay of urban land density (built-up density) in concentric rings reflects the gradient of urban development intensity [19]. Some studies divide concentric rings into multiple sectors to measure the heterogeneity of urban growth in different directions [15]. Considering irregular urban forms or spatial constrains, such as UK's 'green belts' and large water bodies in Wuhan, China, an improved partitioning method for concentric-ring analysis was proposed [12].

The grid-based analysis divides urban areas into regular grids; for example, 1 km grids [26,29–31]. Each grid is a sample and the urban dynamics in each grid are different, which determines the overall spatial pattern of land-use transformation. Grid-based analysis allows the correlation analysis between urban land and other occupied land, and it also builds the bridge between urban land expansion and population growth [26]. The growth in population fundamentally drives the expansion of urbanized land [32]. Numerous studies reported the faster growth rate of urban land than that of population over time, resulting in a decline in the urban population density [33–40].

In this study, we attempt to combine the concentric-ring analysis and grid-based analysis to quantify spatio-temporal characteristics of urban expansion. Our case study area is Latin America, defined as the Americas south of the United States. Latin America consists of 20 countries and 13 dependencies, with more than 640 million population in 2016 and an area of approximately 19,000,000 km^2. In many countries of Latin America, the economy developed rapidly after the middle of the 20th century, and the level of urbanization has continued to increase. Latin America is one of the most urbanized continents in the world with almost 84% of the total population living in cities [41]. For example, Brazil's urbanization level is more than 85%, and Argentina's urbanization level is even more than 90% [42].

Although the urbanization level in Latin America is relatively high, compared with the extensive research of urban expansion in the United States and Europe, there are few studies on the temporal and spatial characteristics of urban expansion in Latin America [41]. In particular, there is a lack of comparative analysis of urban expansion and spatial dynamics among cities in Latin America [13,41,43]. Investigating the dynamics of urban land expansion in Latin America not only has regional significance, but also has international comparative value. It also provides precedents for developing countries that are undergoing rapid urbanization, such as Africa and Asia [44,45].

2. Materials and Methods

2.1. Study Area

New York University, United Nations-Habitat, and Lincoln Institute of Land Policy have published *The Atlas of Urban Expansion* (2016 Edition) of 200 cities around the world, which includes 26 cities in Latin America and the Caribbean [46,47]. Considering the representativeness of large cities and the evenness of their spatial distributions, we selected five large cities with a population of more than five million in 2014 from 26 cities, namely,

São Paulo (Brazil), Mexico City (Mexico), Buenos Aires (Argentina), Bogotá (Colombia), and Santiago (Chile) (Figure 1, Table 1).
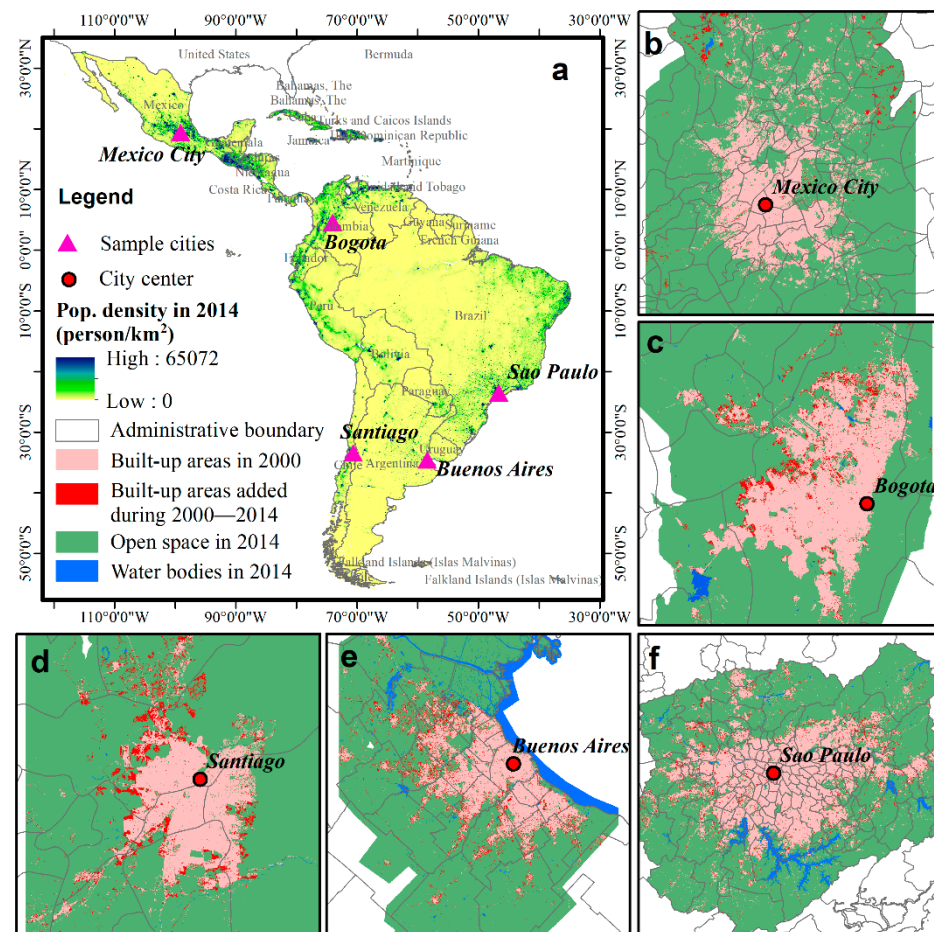
Figure 1. Spatial distributions of five major cities in Latin America with their urban land use in 2000 and 2014.

Table 1. Urban population, built-up area, and population density in 2014 and their annual growth rates from 2000 to 2014 in five large Latin American cities.

City	City Center	Urban Population in 2014 (Million) [#]	AGR [*] of Urban Population (2000–2014, %)	Built-up Area in 2014 (km²) [#]	AGR [*] of Built-up Area (2000–2014, %)	Population Density in 2014 (Person/km²) [#]	AGR [*] of Population Density (2000–2014, %)
São Paulo, Brazil	Catedral Metropolitana de São Paulo	19.61	1.08	1724	0.70	11,372	0.38
Mexico City, Mexico	Palacio Nacional	17.77	2.53	1618	3.56	10,978	−0.99
Buenos Aires, Argentina	Parque centenario	13.88	1.46	1473	1.88	9421	−0.41
Bogotá, Colombia	Museo Nacional	7.80	2.29	319	1.26	24,460	1.02
Santiago, Chile	Plaza Baquedano	6.49	1.32	604	1.76	10,742	−0.43

[#] Data source: The atlas of urban expansion (2016 Edition) http://www.atlasofurbanexpansion.org/ (accessed on 20 April 2021). [*] AGR (annual growth rate) is calculated as $AGR = \left(\sqrt[n]{P_{2014}/P_{2000}} - 1 \right) \cdot 100\%$, where P is the population, built-up area, or population density of a city, and n is the interval in years.

São Paulo is the largest city in Brazil and the economic, cultural, and technological center. Nearly 20 million people lived in São Paulo in 2014 with the total built-up area

being around 1700 km^2. Mexico City is the capital of Mexico and is located in the valley of the plateau of central Mexico, at an altitude over 2000 m. It is the political, economic, cultural and transportation center of Mexico. Buenos Aires is the capital and largest city of Argentina and it is a coastal city on the southern bank of the La Plata River. Bogotá is the capital and largest city in Colombia and it is located in the center of Colombia, on a high plateau known as the Bogotá savanna. Due to the eastern mountains, Bogotá can only expand to the west (Figure 1c). Santiago is the capital and largest city in Chile, which is entirely located in the country's central valley. We identified city centers for the five cities using road maps and high resolution images from Google Map (Figure 1, Table 1).

2.2. Land Use and Population Data

We collected urban land use maps of five Latin American cities in 2000 and 2014 from *The Atlas of Urban Expansion* (*2016 Edition*), which were interpreted using Landsat imagery (30 m resolution) [46]. They classified land use into three categories, namely, built-up area, open space, and water bodies, using the unsupervised classification method (clustering analysis) with the ISODATA (Iterative Self-Organizing Data Analysis Technique) algorithm. The classification result has a high accuracy with verification using Google Earth high resolution imagery. The user's accuracy for the built-up area is 91% and the producer's accuracy is 89.3% [46]. Detailed information on the land use classification procedures can be found in Hurd [48]. The data from *The Atlas of Urban Expansion* (*2016 Edition*) has been successfully used in related studies on urban expansion and urban form [49–51]. The spatial distributions of urban land in 2000 and 2014 and open space and water bodies in 2014 of five Latin American cities are shown in Figure 1.

The population data in Table 1 also comes from *The Atlas of Urban Expansion* (*2016 Edition*), but it is statistical data without information on its spatial distribution. We further collected *LandScan* population data for the five sample cities in 2000 and 2014. *LandScan* is a community standard for global population distribution data at approximately 1 km (30″ × 30″) spatial resolution, and it represents an ambient population (average over 24 h) distribution [52–54]. The spatial distribution of population data supports the correlation analysis between urban expansion and population growth using grid-based analysis.

2.3. Concentric Ring and Grid-Based Analysis

We generate a series of 1-km equidistant buffer rings to cover almost the entire built-up areas in 2014 (Figure 2a). Previous studies calculated landscape metrics in concentric rings and analyze their spatial variations [15]. In this study, we calculate the urban land density (built-up density) in each concentric ring, and then fit its distance decay using the inverse *S* curve (See Section 2.4). The urban land density is defined as the proportion of urban land to the area of buildable land in each ring (Equation (1)).

$$Dens = \frac{S_{urban\ land}}{S_{buildable\ land}} \tag{1}$$

where *Dens* is the urban land density in a concentric ring (doughnut). $S_{urban\ land}$ is the area of urban land (built-up area) in a ring, and $S_{buidable\ land}$ is the area of buildable land in a ring. The buildable land is the total land area excluding water bodies and mountains in a ring. The concentric rings are developed and urban land density in each ring are calculated in ArcGIS 10.6 (ESRI, Inc., Redwoodds, CA, USA).

The unit of grid-based analysis is 1 km, which is consistent with the resolution of *LandScan* population data. We first clip the *LandScan* population data in 2000 and 2014 for each city using the spatial extent of land use map of the same city (Figure 2b). We convert the population raster file to a vector file in 1 km × 1 km grid segments. We calculate the area of built-up area in each grid for two years, 2000 and 2014, using zonal statistics, and then calculate the change of built-up area in each grid from 2000 to 2014. Finally, we use map algebra to calculate the change in population from 2000 to 2014 in each grid of each city and convert the result to a vector file. We combine the changes in built-up areas and

population for the 2000–2014 period based on the ID of each grid. All of these spatial analytics, such as format conversion, zonal statistics, and map algebra, are conducted in ArcGIS 10.6 (ESRI, Inc., Redwoodds, CA, USA).
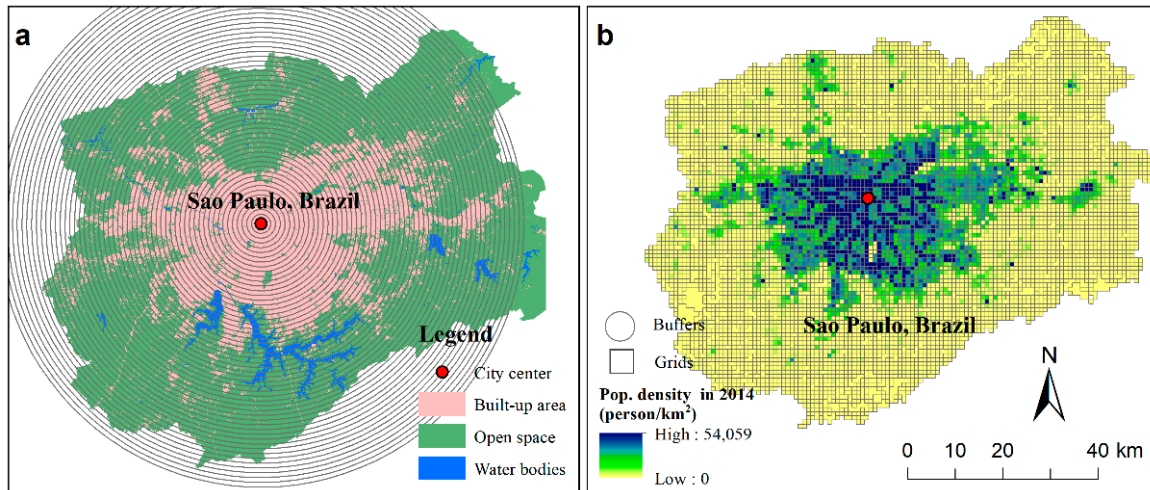

Figure 2. An example of concentric ring analysis (**a**) and grid-based analysis (**b**) in São Paulo, Brazil.

2.4. Inverse S Curve

Jiao (2015) proposed a function with an inverse *S* curve (Figure 3) to characterize the spatial distribution of the urban land density within a city, as shown in Equation (2) [19]:

$$f(r) = \frac{1-c}{1 + e^{\alpha((2r/D)-1)}} + c \tag{2}$$

where *f* is the urban land density (built-up density) in each concentric ring that is calculated using Equation (1), *r* is the distance to the city center, *e* is the Euler's number, and α, *c* and *D* are parameters, which vary across cities and over time.
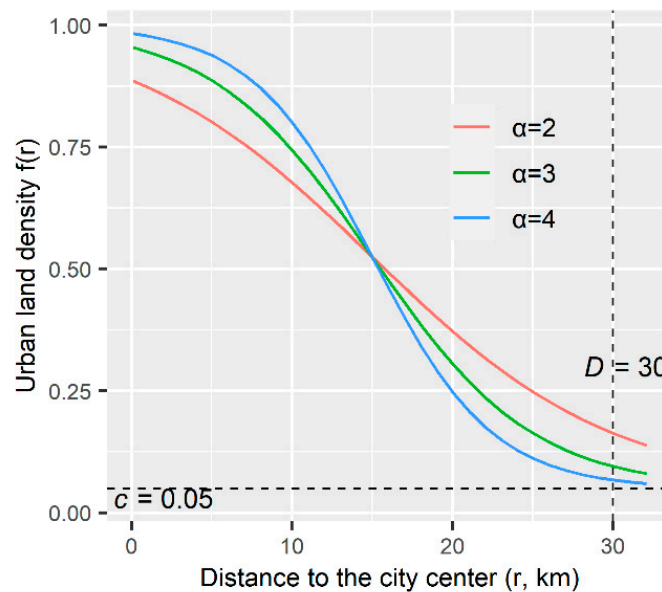

Figure 3. Curves of the urban land density function with different α parameters.

Parameters in the inverse S curve have explicit physical meanings. The α parameter controls the form of the fitting curve and a higher α indicates a more compact urban form (Figure 3). The *D* parameter denotes the approximate boundary of an urban extent. The *c*

parameter represents the background value of the urban land density. The *D* parameter generally increases over time because the urban extent expands. Detailed explanations of these three parameters can be found in Jiao (2015) [19].

The inverse S curve has been an effective and quantitative tool in urban studies. It can be used to not only fit the distance decay of urban land density but also can be applied to other urban indicators, such as the population density, road density, and even land surface temperature (LST) [19,55,56]. The inverse S curve was first proposed using Chinese cities and then it has been applied to cities in other countries across the world [57–60].

3. Results

3.1. Distance Decay of Urban Land Density

We calculate the urban land density in each concentric ring using Formula (1). Overall, the urban land density decreases slowly around the city center, and then decreases quickly to a relatively low level, and finally decreases slowly again to the background level of urban land density, showing an inverse *S*-shape (Figure 4). The inverse S curve can fit the distance decay of urban land density very well in all cities in both 2000 and 2014. Parameters for fitted curves are shown in Table 2. The urban physical size varies among the five cities. The radius of the urban extent (represented by the *D* parameter) is the largest for Buenos Aires, which is over 50 km. The radii of urban extents of São Paulo and Mexico City are around 45 km and 42 km in 2014, respectively. The space size is relatively small for Bogotá and Santiago with urban extent radii of 27 km and 26 km, respectively, in 2014.
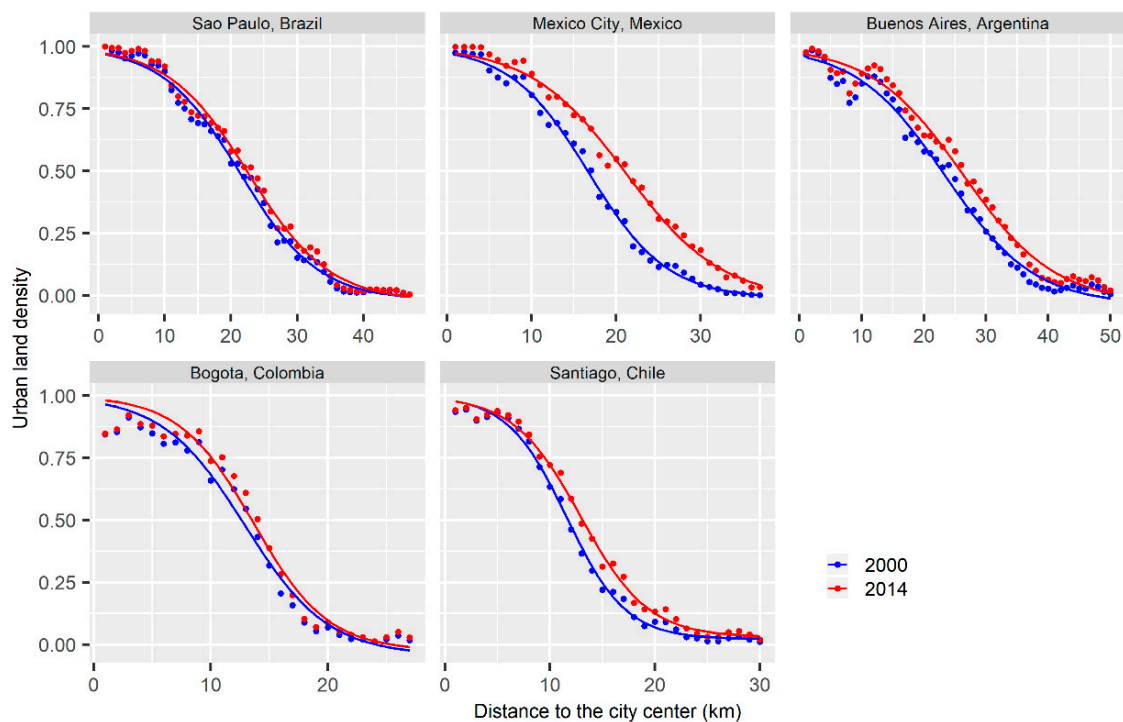
Figure 4. Distance decay of urban land density and fitted results using inverse S curve in concentric rings in five Latin American cities in 2000 and 2014.

The *α* parameter reflects the compactness of urban form and a higher *α* means a more compact urban form. Bogotá has the highest value of *α* (=4.49) in 2014, indicating the most compact urban form among the five cities. The urban population density in Bogotá in 2014 is also the highest among the five cities (24,460 person/km^2, Table 1), further supporting its compact form. Generally, the *α* parameter increases from 2000 to 2014 in four cities except for Santiago, which has a small decline. Cross-sectionally, Buenos Aires has the lowest value of *α*, indicating that it has the most relatively dispersed urban form.

The urban population density in Buenos Aires is also the lowest among the five cities (9421 person/km^2, Table 1).

Table 2. Parameters of the inverse S curve for five Latin American cities in 2000 and 2014.

City	Year	Num. of Rings	α	c	D	Adjusted R^2
São Paulo	2000	47	3.70	0.01	42.11	0.993
	2014	47	3.83	0.03	44.51	0.992
Mexico city	2000	37	3.65	0.02	33.12	0.996
	2014	37	3.78	0.03	41.73	0.994
Buenos Aires	2000	50	3.39	0.01	45.38	0.987
	2014	50	3.70	0.04	51.43	0.988
Bogotá	2000	27	3.87	0.03	25.13	0.974
	2014	27	4.49	0.05	26.95	0.976
Santiago	2000	30	4.11	0.02	23.17	0.996
	2014	30	4.03	0.03	25.82	0.996

The gap between the two curves of the same city for 2000 and 2014 reflects the dynamics of the urban expansion, which varies among the five cities. Mexico City has the largest gap between the two curves, indicating the most obvious urban expansion in this city. Comparatively, the two curves of São Paulo nearly overlap, implying a limited urban expansion in this city. The gap between the two curves also reflects the spatial disparities in urban expansion. The new urban land is mainly added around 10 km from the city center in Bogotá from 2000 to 2014, while in Santiago the urban expansion took place in its outskirts. This is why the urban form of Santiago has become more dispersed during 2000–2014 (Table 2). The new urban land is evenly distributed in space in Buenos Aires (Figure 4).

3.2. Directional Heterogeneity in Urban Form

Urban expansion is generally not homogeneous, but there is usually a directional heterogeneity due to the influence of natural conditions or urban planning [15,61]. Taking São Paulo as an example, we divided the concentric ring into four directions, namely East, South, West, and North, as shown in Figure 5a. Due to the limited urban expansion from 2000 to 2014 in São Paulo (Figure 4), we only take the land use information in 2014 to present the heterogeneity of urban form in different directions. Overall, São Paulo has an urban form with a longer-extent in the east-west direction but a more limited extent in a north-south direction, which is restricted by the macro physical geography (mountains in the north and water bodies in the south). The built-up area in the easterly direction is 717 km^2, which is the largest among the four directions, taking 42% of the whole built-up area (1724 km^2, Table 1). The built-up area in the northern direction is only 248 km^2.

We calculate the urban land density in four directions in São Paulo using concentric rings (Figure 5a). There are obvious disparities in the distance decay of urban land density and fitted curves in the four directions (Figure 5b). The parameters for the inverse S curve in the four directions are shown in Table 3. The fitted urban extents (parameter D) are 55 km, 47 km, 47 km, and 27 km in the East, South, West, and North, respectively. Unsurprisingly, the urban extent in the east is the largest, which is more than twice of that in the north. Remember that the α parameter indicates the compactness of urban form. Urban expansion in the south is restricted by water bodies, resulting in the most compact form in this direction ($\alpha = 8.81$), while the urban form is relatively dispersed in the west ($\alpha = 4.37$). There is an obvious bump of the urban land density in the north at around 26 km from the city center, which is caused by leapfrogging urban patches in the north of the city center (Figure 5b).
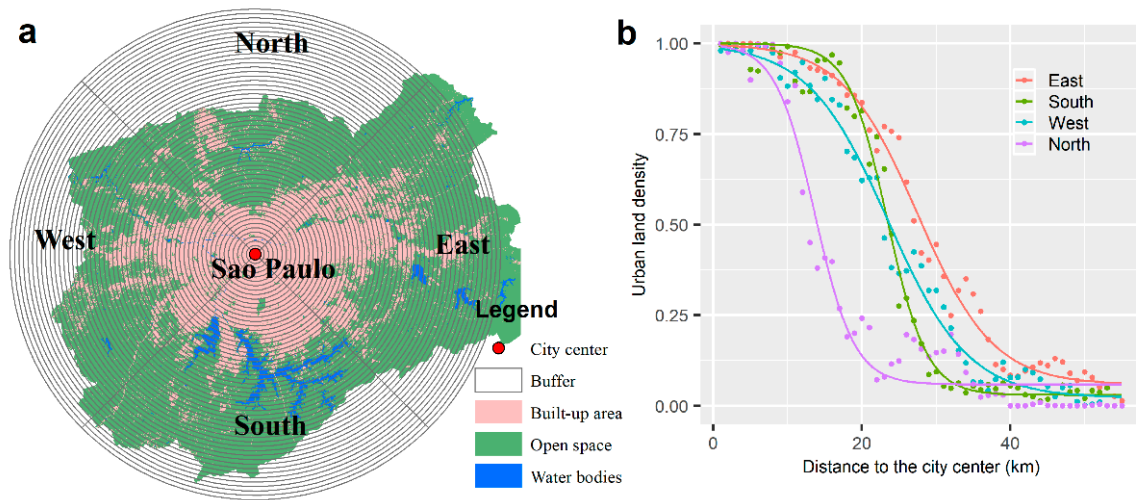
Figure 5. The concentric ring in four directions (**a**) and the spatial attenuation of urban land density in four directions of São Paulo in 2014 (**b**).

**Table 3.** Parameters of inversed-S shape function in four directions of São Paulo.

Directions	α	c	D	Adjusted R^2
East	5.43	0.06	55.02	0.990
South	8.81	0.03	46.83	0.989
West	4.37	0.02	47.05	0.989
North	5.16	0.06	27.36	0.963

3.3. Correlations between Land Expansion and Population Growth

We use grid-based analysis to investigate urban land expansion, population growth and their correlations. Changes in population and built-up areas in 1 km grid squares for 2000 and 2014 are presented in Figure 6. There are apparent disparities in space for both land expansion and population growth. Population increases in some places while it decreases in other locations. Taking São Paulo as an example, the urban population decreased around the city center and urban core area, while it increased in the urban fringe and suburban areas (Figure 6a), reflecting the process of suburbanization [62]. Mexico City, Buenos Aires, and Santiago also experienced the transformation of population from the city center to suburban areas, but with different characteristics (Figure 6b,c,h). In Mexico City, urban population transferred from the east to the west during 2000–2014 (Figure 6b). Although the central part of Buenos Aires had an increased population, the urban population obviously decreased near the city center, forming a doughnut with a reduced population around the center (Figure 6c). The urban population change in Santiago shows the strongest heterogeneity, which declined in the main corridors passing through the city center. Different from the other four cities, there is no obvious decline in population around the city center in Bogotá (Figure 6g).

Generally, the expansion of urban land shares a similar pattern as seen in the population growth. The new built-up areas mainly occurred at the urban fringe and suburban areas, while a limited newly built-up area was found around the city center (Figure 6d–f,i,j). In São Paulo, the urban expansion hotspots are located in the east and west from 2000 to 2014 (Figure 6b). The urban land spread evenly around the city center in Mexico City, particularly in the north and southeast (Figure 6e). As a coastal city, the new urban land can only spread to the inland side of Buenos Aires and most of these lie along main roads (Figure 6f). Bogotá shows a massive urban expansion northwest of the city center (Figure 6i). The urban expansion surrounded the city center of Santiago with more new urban land located in the northwest of the city (Figure 6j).
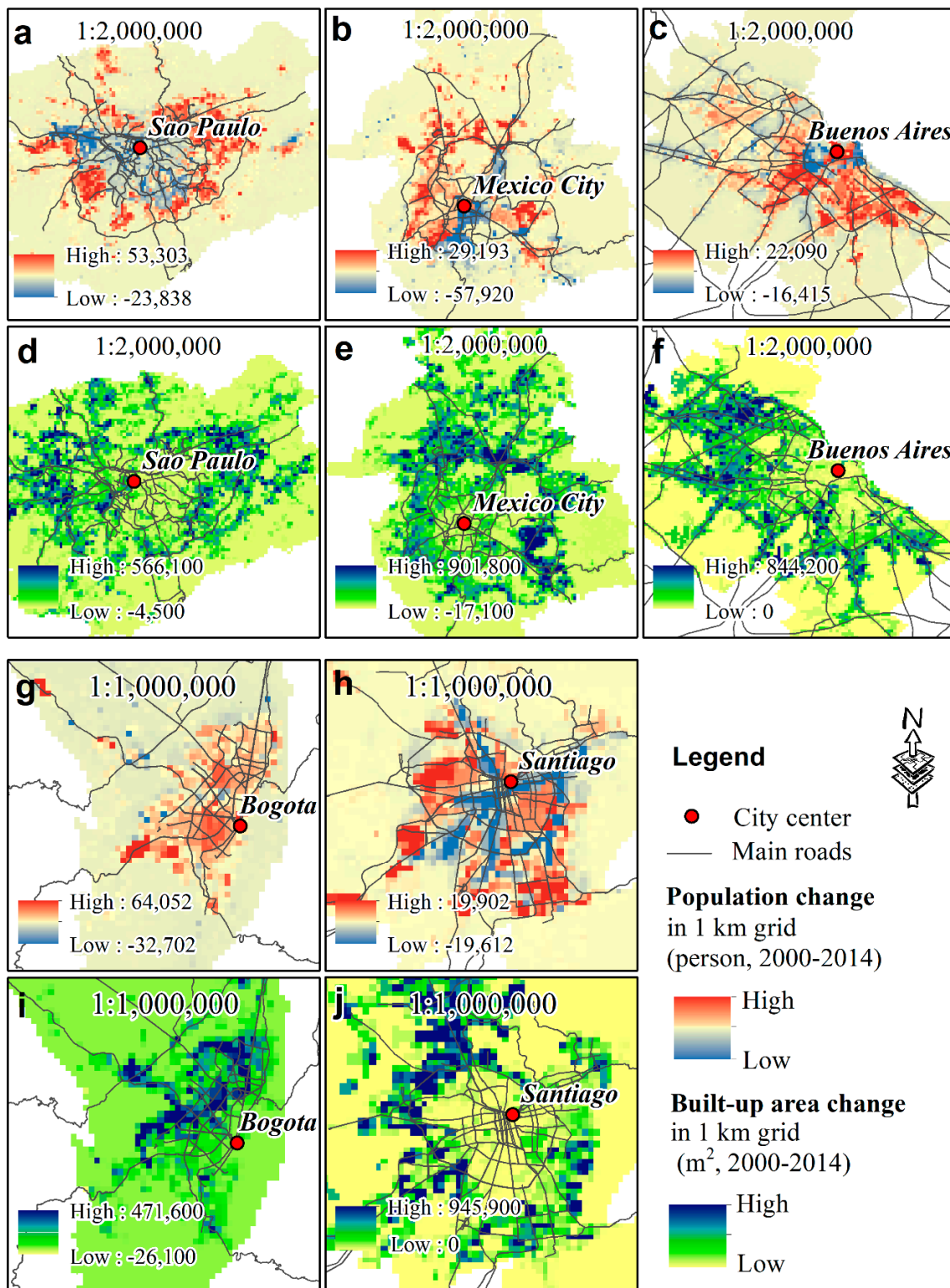
Figure 6. Spatial distributions of population changes (**a–c,g,h**) and built-up area changes (**d–f,i,j**) from 2000 to 2014 in five Latin American cities. Only three types of roads (trunk, primary, motorway) were preserved from the OSM road net (https://www.openstreetmap.org) (accessed on 20 April 2021).

The frequency distributions of changes in population and built-up area from 2000 to 2014 in 1 km grid squares are shown in Figure 7a,b, and their correlations are presented in Figure 7c. Population and built-up areas remain unchanged in most grids during 2000–2014. The mean values of population change in the 1 km grid are 563 persons

(São Paulo), 536 persons (Mexico City), 518 persons (Buenos Aires), 944 persons (Bogotá), and 200 person (Santiago). The mean values of changes in the built-up areas using the 1 km grid are 2.49 hm^2 (São Paulo), 9.88 hm^2 (Mexico City), 4.64 hm^2 (Buenos Aires), 1.96 hm^2 (Bogotá), and 3.15 hm^2 (Santiago). From the mean values for each grid, Bogotá experiences the highest population increase but with the least expansion in use of urban land, verifying its high population density (Tables 1 and 2) and compact urban form. Scatter plots show that the population change and the built-up area change are positively correlated (Figure 7c).
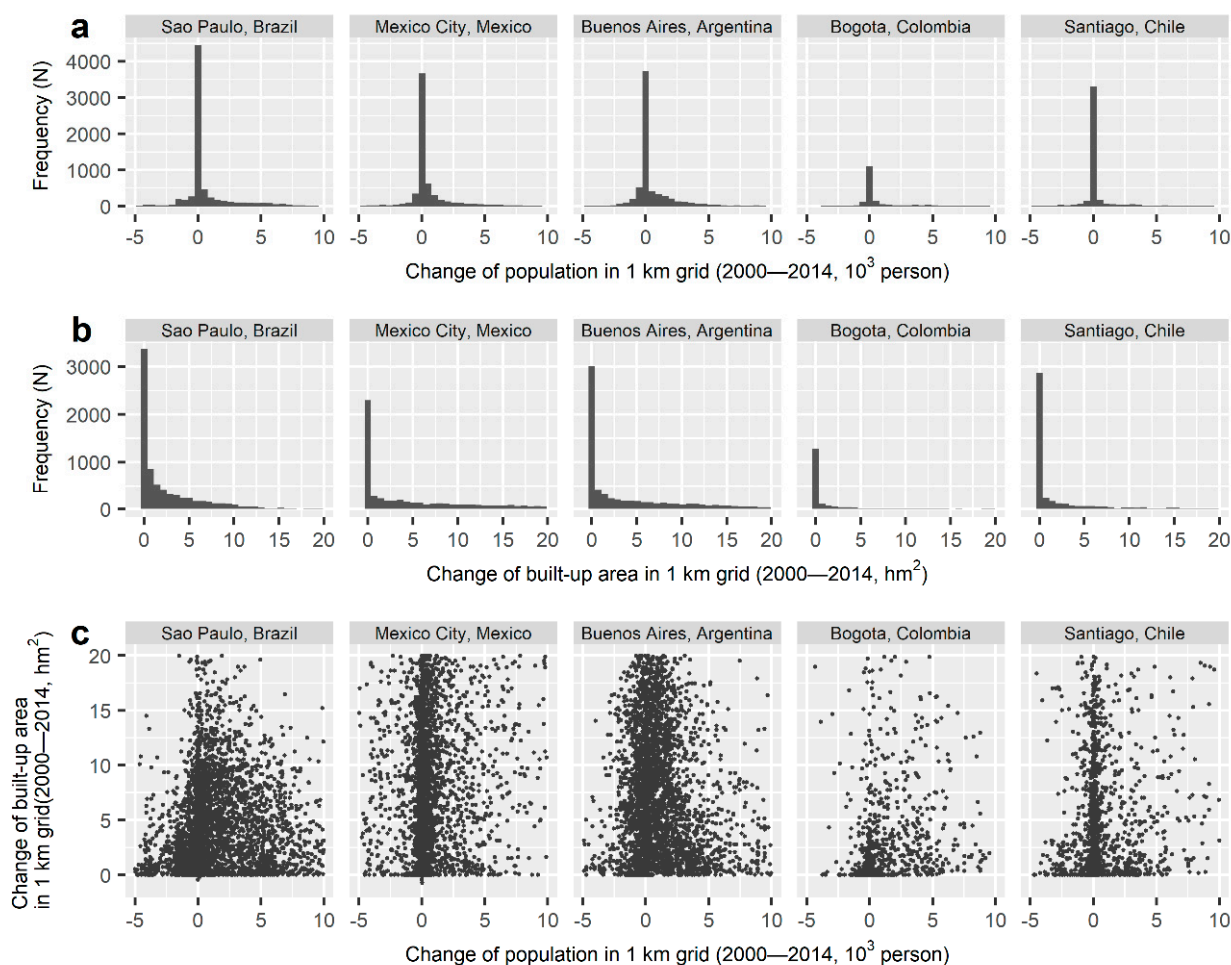
Figure 7. Frequency distribution and correlation analysis between the population growth and the urban land expansion from 2000 to 2014 in five Latin American cities. (**a**) Frequency of population change; (**b**) Frequency of built-up area change; (**c**) Scatter plots of population change and built-up area change in each 1 km grid.

4. Discussion

The city is composed of different spatial units. In addition to administrative divisions, the two most commonly used units in urban studies are concentric-rings and grids. Concentric-ring analysis, also called gradient analysis, is developed based on the monocentric model of cities, which does well in measuring macro pattern (urban-rural gradient) of urban expansion and urban form. Grid-based analysis has advantages in portraying the local microscopic dynamics of urban expansion. Grid-based analysis is usually used to build correlations between urban land and population changes. Urban expansion is a process from micro dynamics to macro patterns. Every land use change occurred in a local area, but the accumulation of local micro-processes shaped the macro pattern of urban expansion. The combined use of concentric-ring and grid-based analysis can measure urban expansion from both macro and micro perspectives. Although the concentric-ring

analysis and grid-based analysis have been used in previous studies, they are all used in a single way. We propose for the first time that these are two different strategies for measuring urban expansion.

We combined these two approaches to quantify urban expansion for five major Latin America cities from 2000 to 2014. The urban land density (built-up density) in concentric rings decreases from the city center to suburban areas, presenting an inverse S-shape (Figure 4). Partitioning concentric rings into different sectors can effectively quantify the directional heterogeneity of urban expansion (Figure 5). The grid-based analysis particularly presents the process of suburbanization where population transferred from central areas to suburban areas from 2000 to 2014 (Figure 6). Meanwhile, the newly added urban land mainly expands in the urban fringe and suburban areas to accommodate the increasing population there (Figure 6).

Parameters of the inverse *S* curve reveal the urban extents and compactness of urban form (Figure 4, Table 2). Although São Paulo has the largest built-up area, Buenos Aires has a larger urban extent than São Paulo. Buenos Aires experienced the most dispersed urban form, while the urban form is the most compact in Bogotá. The compactness of the urban form quantified by the inverse S curve is consistent with urban population densities that is the highest in Bogotá but the lowest in Buenos Aires (Table 1). The calculation of population change and built-up change using the grid-based analysis also confirms that the compact growth in Bogotá, where the urban population averagely increase by 944 person at a cost of 1.96 hm^2 for each 1 km grid during 2000–2014 (Figure 7).

In the global context, the speed of urban land expansion in Latin American cities is relatively low. The intensity of the urban expansion is reflected by the gaps between the two fitting curves using the inverse S curve. The gaps between the two curves in 2000 and 2014 are very close and even overlapped in the five major Latin American cities (Figure 4). Not to mention the fast urban expansion in China and other countries in Asia and Africa, even the expansion of urban land in the United States and Europe is greater than in Latin America [19,44,45,63]. On the other hand, the urban form of Latin American cities is more compact than for cities in other regions, which is quantified by the α parameter of the inverse S curve. The α parameter for the five major Latin American cities varies in 3.39–4.49, while that for Chinese and European cities is around 2.5, and is less than 2 for cities in the United States for the same two years (2000 and 2014) [6,20,44]. Many Latin American cities grow in rugged topographies which constrains expansion, resulting in the overall compact urban form [43].

The distance-decay of urban population densities from the city center has long been revealed in urban geography and urban economics [64]. Classical models include the Clark's negative exponential model [64], the Batty's inverse power function [65] and many other models [66]. The urban land density, defined as the proportion of built-up areas to the buildable land in concentric rings, also declines with distance to the city center, but there are limited quantitative models to measure this process [28]. Urban land density declines slowly around the city center followed by a quick decline outward, and then declines slowly again in the urban periphery, showing an inverse *S* shape as a whole [19]. Inspired by the widely used sigmoid function with an *S* curve, Jiao (2015) proposed an inverse *S* curve to quantify the distance-decay of urban land density from the city center [19]. The urban land density function (inverse S curve) has been not only used to quantify past urban expansion but also to guide the spatial allocation of future urban land, which has potential applications in urban planning [67]. Recently, a geographic micro-process model was proposed to explain why the distance-decay of urban land density presents an inverse S shape [20].

This study also has limitations. This study only quantifies the growth of cities from a spatial perspective, neglecting the underlying driving forces of urban transformation [25]. Secondly, we chose the city center based on the road network and we only identified one city center for each city. With the development of cities, those large cities tend to be polycentric. There are slight bumps of urban land densities around 12 km from the

city center in Buenos Aires (Figure 4). These bumps are closely related to the polycentric structure of cities, which can be controlled using polycentric scenarios in concentric ring partitioning [19,45]. In addition, the intervals (1 km, 2 km, and so on) in concentric-ring analysis and the size of grids (1 × 1 km, 2 × 2 km, and so on) have an effect of scale [68], which is not further discussed in this study.

5. Conclusions

This study contributes to the characterization of urban expansion by summarizing two approaches: Concentric-ring analysis and grid-based analysis. Concentric-ring analysis is developed based on the monocentric model of cities and it is easy to present the distance decay of urban elements from the city center to suburban areas. Grid-based analysis partitions a city into regular grids, which reflects local dynamics of urban growth.

Taking five major cities in Latin America as examples, this study combines concentric-ring analysis and grid-based analysis to quantify their urban expansion and population growth from 2000 to 2014. Urban land density in concentric rings declines with the distance from the city center. The inverse *S* curve not only can well fit the distance decay of densities but also reflects disparities in the urban extent and compactness of the urban form. Grid-based analysis characterizes the transformation of population from central areas to suburban areas. It is suggested to combine concentric-ring and grid-based analysis to fully quantify urban expansion from both perspectives of macro patterns and micro dynamics in other global cities.

Author Contributions: Conceptualization, G.X. and S.W.; methodology, S.W., T.D., and G.X.; software, S.W.; data curation, S.W.; writing—original draft preparation, S.W. and G.X.; writing—review and editing, N.S.S., T.D., G.X. and Y.L. All authors have read and agreed to the published version of the manuscript.

Institutional Review Board Statement: Not applicable.

Informed Consent Statement: Not applicable.

Data Availability Statement: Data used in this study is publicly available. Land use maps retrieved from Landsat images are downloaded from http://www.atlasofurbanexpansion.org/ (accessed on 20 April 2021). The spatial distributions of population are downloaded from https://landscan.ornl.gov/ (accessed on 20 April 2021).

Conflicts of Interest: The authors declare no conflict of interest.

References

1. Van Vliet, J. Direct and indirect loss of natural area from urban expansion. *Nat. Sustain.* **2019**, *2*, 755–763. [CrossRef]
2. Bren d'Amour, C.; Reitsma, F.; Baiocchi, G.; Barthel, S.; Guneralp, B.; Erb, K.H.; Haberl, H.; Creutzig, F.; Seto, K.C. Future urban land expansion and implications for global croplands. *Proc. Natl. Acad. Sci. USA* **2017**, *114*, 8939–8944. [CrossRef] [PubMed]
3. Yang, C.; Liu, H.; Li, Q.; Cui, A.; Xia, R.; Shi, T.; Zhang, J.; Gao, W.; Zhou, X.; Wu, G. Rapid Urbanization Induced Extensive Forest Loss to Urban Land in the Guangdong-Hong Kong-Macao Greater Bay Area, China. *Chin. Geogr. Sci.* **2021**, *31*, 93–108. [CrossRef]
4. Yang, Q.; Huang, X.; Yang, J.; Liu, Y. The relationship between land surface temperature and artificial impervious surface fraction in 682 global cities: Spatiotemporal variations and drivers. *Environ. Res. Lett.* **2021**, *16*, 024032. [CrossRef]
5. Xia, C.; Zhang, A.; Wang, H.; Zhang, B.; Zhang, Y. Bidirectional urban flows in rapidly urbanizing metropolitan areas and their macro and micro impacts on urban growth: A case study of the Yangtze River middle reaches megalopolis, China. *Land Use Policy* **2019**, *82*, 158–168. [CrossRef]
6. Dong, T.; Jiao, L.; Xu, G.; Yang, L.; Liu, J. Towards sustainability? Analyzing changing urban form patterns in the United States, Europe, and China. *Sci. Total Environ.* **2019**, *671*, 632–643. [CrossRef]
7. Hailemariam, S.N.; Soromessa, T.; Teketay, D. Land Use and Land Cover Change in the Bale Mountain Eco-Region of Ethiopia during 1985 to 2015. *Land* **2016**, *5*, 41. [CrossRef]
8. Liu, X.; Hu, G.; Chen, Y.; Li, X.; Xu, X.; Li, S.; Pei, F.; Wang, S. High-resolution multi-temporal mapping of global urban land using Landsat images based on the Google Earth Engine Platform. *Remote Sens. Environ.* **2018**, *209*, 227–239. [CrossRef]

9. Xiao, J.; Shen, Y.; Ge, J.; Tateishi, R.; Tang, C.; Liang, Y.; Huang, Z. Evaluating urban expansion and land use change in Shijiazhuang, China, by using GIS and remote sensing. *Landsc. Urban Plan.* **2006**, *75*, 69–80. [CrossRef]
10. Xu, X.; Min, X. Quantifying spatiotemporal patterns of urban expansion in China using remote sensing data. *Cities* **2013**, *35*, 104–113. [CrossRef]
11. Zhao, S.; Zhou, D.; Zhu, C.; Sun, Y.; Wu, W.; Liu, S. Spatial and temporal dimensions of urban expansion in China. *Environ. Sci. Technol.* **2015**, *49*, 9600–9609. [CrossRef] [PubMed]
12. Jiao, L.; Xu, G.; Xiao, F.; Liu, Y.; Zhang, B. Analyzing the Impacts of Urban Expansion on Green Fragmentation Using Constraint Gradient Analysis. *Prof. Geogr.* **2017**, *69*, 553–566. [CrossRef]
13. Schneider, A.; Woodcock, C.E. Compact, Dispersed, Fragmented, Extensive? A Comparison of Urban Growth in Twenty-five Global Cities using Remotely Sensed Data, Pattern Metrics and Census Information. *Urban Stud.* **2008**, *45*, 659–692. [CrossRef]
14. Herold, M.; Goldstein, N.C.; Clarke, K.C. The spatiotemporal form of urban growth: Measurement, analysis and modeling. *Remote Sens. Environ.* **2003**, *86*, 286–302. [CrossRef]
15. Ramachandra, T.V.; Aithal, B.H.; Sanna, D.D. Insights to urban dynamics through landscape spatial pattern analysis. *Int. J. Appl. Earth Obs. Geoinf.* **2012**, *18*, 329–343.
16. He, Q.; Song, Y.; Liu, Y.; Yin, C. Diffusion or coalescence? Urban growth pattern and change in 363 Chinese cities from 1995 to 2015. *Sustain. Cities Soc.* **2017**, *35*, 729–739. [CrossRef]
17. Dietzel, C.; Oguz, H.; Hemphill, J.J.; Clarke, K.C.; Gazulis, N. Diffusion and coalescence of the Houston Metropolitan Area: Evidence supporting a new urban theory. *Environ. Plan. B Plan. Des.* **2005**, *32*, 231–246. [CrossRef]
18. Herold, M.; Hemphill, J.; Dietzel, C.; Clarke, K. Remote sensing derived mapping to support urban growth theory. In Proceedings of the 3rd International Symposium Remote Sensing and Data Fusion over Urban Areas (URBAN 2005) and 5th International Symposium Remote Sensing of Urban Areas (URS 2005), Tempe, AZ, USA, 1 March 2005.
19. Jiao, L. Urban land density function: A new method to characterize urban expansion. *Landsc. Urban Plan.* **2015**, *139*, 26–39. [CrossRef]
20. Jiao, L.; Dong, T.; Xu, G.; Zhou, Z.; Liu, J.; Liu, Y. Geographic micro-process model: Understanding global urban expansion from a process-oriented view. *Comput. Environ. Urban Systems* **2021**, *87*, 101603. [CrossRef]
21. Liu, X.; Li, X.; Chen, Y.; Tan, Z.; Li, S.; Ai, B. A new landscape index for quantifying urban expansion using multi-temporal remotely sensed data. *Landsc. Ecol.* **2010**, *25*, 671–682. [CrossRef]
22. Liu, J.; Jiao, L.; Zhang, B.; Xu, G.; Yang, L.; Dong, T.; Xu, Z.; Zhong, J.; Zhou, Z. New indices to capture the evolution characteristics of urban expansion structure and form. *Ecol. Indic.* **2021**, *122*, 107302. [CrossRef]
23. Jiao, L.; Liu, J.; Xu, G.; Dong, T.; Gu, Y.; Zhang, B.; Liu, Y.; Liu, X. Proximity Expansion Index: An improved approach to characterize evolution process of urban expansion. *Comput. Environ. Urban Syst.* **2018**, *70*, 102–112. [CrossRef]
24. Jiao, L.; Mao, L.; Liu, Y. Multi-order landscape expansion index: Characterizing urban expansion dynamics. *Landsc. Urban Plan.* **2015**, *137*, 30–39. [CrossRef]
25. Brueckner, J.K. Urban sprawl: Diagnosis and remedies. *Int. Reg. Sci. Rev.* **2000**, *23*, 160–171. [CrossRef]
26. Bagan, H.; Yamagata, Y. Landsat analysis of urban growth: How Tokyo became the world's largest megacity during the last 40 years. *Remote Sens. Environ.* **2012**, *127*, 210–222. [CrossRef]
27. Seto, K.C.; Fragkias, M. Quantifying spatiotemporal patterns of urban land-use change in four cities of China with time series landscape metrics. *Landsc. Ecol.* **2005**, *20*, 871–888. [CrossRef]
28. Guérois, M.; Pumain, D. Built-Up Encroachment and the Urban Field: A Comparison of Forty European Cities. *Environ. Plan. A Econ. Space* **2008**, *40*, 2186–2203. [CrossRef]
29. Bagan, H.; Yamagata, Y. Land-cover change analysis in 50 global cities by using a combination of Landsat data and analysis of grid cells. *Environ. Res. Lett.* **2014**, *9*, 0640155. [CrossRef]
30. Maimaitijiang, M.; Ghulam, A.; Sandoval, J.O.; Maimaitiyiming, M. Drivers of land cover and land use changes in St. Louis metropolitan area over the past 40 years characterized by remote sensing and census population data. *Int. J. Appl. Earth Obs. Geoinf.* **2015**, *35*, 161–174. [CrossRef]
31. Hou, H.; Estoque, R.C.; Murayama, Y. Spatiotemporal analysis of urban growth in three African capital cities: A grid-cell-based analysis using remote sensing data. *J. Afr. Earth Sci.* **2016**, *123*, 381–391. [CrossRef]
32. Colsaet, A.; Laurans, Y.; Levrel, H. What drives land take and urban land expansion? A systematic review. *Land Use Policy* **2018**, *79*, 339–349. [CrossRef]
33. Angel, S.; Parent, J.; Civco, D.L.; Blei, A.M. *The Persistent Decline in Urban Densities: Global and Historical Evidence of Sprawl*; Working Paper; Lincoln Institute of Land Policy: Cambridge, MA, USA, 2010.
34. Seto, K.C.; Fragkias, M.; Guneralp, B.; Reilly, M.K. A meta-analysis of global urban land expansion. *PLoS ONE* **2011**, *6*, e23777. [CrossRef]
35. Haase, D.; Kabisch, N.; Haase, A. Endless urban growth? On the mismatch of population, household and urban land area growth and its effects on the urban debate. *PLoS ONE* **2013**, *8*, e66531. [CrossRef]
36. Kasanko, M.; Barredo, J.I.; Lavalle, C.; McCormick, N.; Demicheli, L.; Sagris, V.; Brezger, A. Are European cities becoming dispersed? A comparative analysis of 15 European urban areas. *Landsc. Urban Plan.* **2006**, *77*, 111–130. [CrossRef]
37. Güneralp, B.; Reba, M.; Hales, B.U.; Wentz, E.A.; Seto, K.C. Trends in urban land expansion, density, and land transitions from 1970 to 2010: A global synthesis. *Environ. Res. Lett.* **2020**, *15*, 044015. [CrossRef]

38. Xu, G.; Jiao, L.; Yuan, M.; Dong, T.; Zhang, B.; Du, C. How does urban population density decline over time? An exponential model for Chinese cities with international comparisons. *Landsc. Urban Plan.* **2019**, *183*, 59–67. [CrossRef]

39. Xu, G.; Zhou, Z.; Jiao, L.; Zhao, R. Compact Urban Form and Expansion Pattern Slow Down the Decline in Urban Densities: A Global Perspective. *Land Use Policy* **2020**, *94*, 104563. [CrossRef]

40. Song, X.; Feng, Q.; Xia, F.; Li, X.; Scheffran, J. Impacts of changing urban land-use structure on sustainable city growth in China: A population-density dynamics perspective. *Habitat Int.* **2021**, *107*, 102296. [CrossRef]

41. Inostroza, L.; Baur, R.; Csaplovics, E. Urban sprawl and fragmentation in Latin America: A dynamic quantification and characterization of spatial patterns. *J. Environ. Manag.* **2013**, *115*, 87–97. [CrossRef] [PubMed]

42. WorldBank. Data bank. Available online: https://data.worldbank.org/indicator (accessed on 16 March 2021).

43. Duque, J.C.; Lozano-Gracia, N.; Patino, J.E.; Restrepo, P.; Velasquez, W.A. Spatio-Temporal Dynamics of Urban Growth in Latin American Cities: An Analysis Using Nighttime Lights Imagery. *Landsc. Urban Plan.* **2019**, *191*. [CrossRef]

44. Xu, G.; Dong, T.; Cobbinah, P.B.; Jiao, L.; Sumari, N.S.; Chai, B.; Liu, Y. Urban expansion and form changes across African cities with a global outlook: Spatiotemporal analysis of urban land densities. *J. Clean. Prod.* **2019**, *224*, 802–810. [CrossRef]

45. Xu, G.; Jiao, L.; Liu, J.; Shi, Z.; Zeng, C.; Liu, Y. Understanding urban expansion combining macro patterns and micro dynamics in three Southeast Asian megacities. *Sci. Total Environ.* **2019**, *660*, 375–383. [CrossRef]

46. Angel, S.; Blei, A.M.; Parent, J.; Lamson-Hall, P.; Sanchez, N.G. *Atlas of Urban. Expansion—2016 Edition*; Areas and Densities; New York University: New York, NY, USA; UN-Habitat: Nairobi, Kenya; Lincoln Institute of Land Policy: Cambridge, MA, USA, 2016; Volume 1.

47. Atlas of Urban Expansion. Available online: http://www.atlasofurbanexpansion.org/ (accessed on 16 March 2021).

48. Hurd, J. *Atlas of Global Expansion 2015 Edition Cities Classification Procedures Manual*; University of Connecticut: Storrs, CT, USA, 2015.

49. Angel, S.; Lamson-Hall, P.; Blei, A.; Shingade, S.; Kumar, S. Densify and Expand: A Global Analysis of Recent Urban Growth. *Sustainability* **2021**, *13*, 3835. [CrossRef]

50. Angel, S.; Arango Franco, S.; Liu, Y.; Blei, A.M. The shape compactness of urban footprints. *Prog. Plan.* **2020**, *139*, 100429. [CrossRef]

51. Lemoine-Rodríguez, R.; Inostroza, L.; Zepp, H. The global homogenization of urban form. An assessment of 194 cities across time. *Landsc. Urban Plan.* **2020**, *204*, 103949. [CrossRef]

52. Landscan. Available online: https://landscan.ornl.gov/ (accessed on 16 March 2021).

53. Bright, E.A.; Coleman, P.R. *LandScan 2000*; Oak Ridge National Laboratory: Oak Ridge, TN, USA, 2001.

54. Bright, E.A.; Rose, A.N.; Urban, M.L. *LandScan 2014*; Oak Ridge National Laboratory: Oak Ridge, TN, USA, 2015.

55. Xiao, R.; Tian, Y.; Xu, G. Spatial gradient of urban green field influenced by soil sealing. *Sci. Total Environ.* **2020**, *735*, 139490. [CrossRef] [PubMed]

56. Bonafoni, S.; Keeratikasikorn, C. Land surface temperature and urban density: Multiyear modeling and relationship analysis using MODIS and Landsat data. *Remote Sens.* **2018**, *10*, 1471. [CrossRef]

57. Sumari, N.S.; Cobbinah, P.B.; Ujoh, F.; Xu, G. On the absurdity of rapid urbanization: Spatio-temporal analysis of land-use changes in Morogoro, Tanzania. *Cities* **2020**, *107*, 102876. [CrossRef]

58. Sumari, N.S.; Xu, G.; Ujoh, F.; Korah, P.I.; Ebohon, O.J.; Lyimo, N.N. A Geospatial Approach to Sustainable Urban Planning: Lessons for Morogoro Municipal Council, Tanzania. *Sustainability* **2019**, *11*, 6508. [CrossRef]

59. Govind, N.R.; Ramesh, H. Exploring the relationship between LST and land cover of Bengaluru by concentric ring approach. *Environ. Monit. Assess.* **2020**, *192*, 1–25. [CrossRef] [PubMed]

60. Keeratikasikorn, C. A comparative study on four major cities in Northeastern Thailand using urban land density function. *Geo-Spat. Inf. Sci.* **2018**, *21*, 93–101. [CrossRef]

61. Li, X.; Zhang, L.; Liang, C. A GIS-based buffer gradient analysis on spatiotemporal dynamics of urban expansion in Shanghai and its major satellite cities. *Procedia Environ. Sci.* **2010**, *2*, 1139–1156. [CrossRef]

62. Mieszkowski, P.; Mills, E.S. The causes of metropolitan suburbanization. *J. Econ. Perspect.* **1993**, *7*, 135–147. [CrossRef]

63. Chai, B.; Seto, K.C. Conceptualizing and characterizing micro-urbanization: A new perspective applied to Africa. *Landsc. Urban Plan.* **2019**, *190*, 103595. [CrossRef]

64. Clark, C. Urban population densities. *J. R. Stat. Soc.* **1951**, *114*, 490–496. [CrossRef]

65. Batty, M.; Sik Kim, K. Form follows function: Reformulating urban population density functions. *Urban Stud.* **1992**, *29*, 1043–1069. [CrossRef]

66. Zielinski, K. Experimental analysis of eleven models of urban population density. *Environ. Plan. A* **1979**, *11*, 629–641. [CrossRef] [PubMed]

67. Wang, W.; Jiao, L.; Dong, T.; Xu, Z.; Xu, G. Simulating urban dynamics by coupling top-down and bottom-up strategies. *Int. J. Geogr. Inf. Sci.* **2019**, *33*, 2259–2283. [CrossRef]

68. Zhang, B.; Xu, G.; Jiao, L.; Liu, J.; Dong, T.; Li, Z.; Liu, X.; Liu, Y. The scale effects of the spatial autocorrelation measurement: Aggregation level and spatial resolution. *Int. J. Geogr. Inf. Sci.* **2019**, *33*, 945–966. [CrossRef]